Imprint of galaxy formation and evolution on globular cluster properties

Kenji Bekki

School of Physics, University of New South Wales, Sydney 2052, Australia
bekki@bat.phys.unsw.edu.au

Summary. We discuss the origin of physical properties of globular cluster systems (GCSs) in galaxies in terms of galaxy formation and evolution processes. Based on numerical simulations of dynamical evolution of GCSs in galaxies, we particularly discuss (1) the origin of radial density profiles of GCSs, (2) kinematics of GCSs in elliptical galaxies, (3) transformation from nucleated dwarf galaxies into GCs (e.g., omega Centauri), and (4) the origin of GCSs in the Large Magellanic Cloud (LMC).

1 Numerical archeology

Based on penetrative analysis of metal-poor halo stars and globular clusters (GCs) in the Galaxy, two canonical Galaxy formation scenarios – the monolithic collapse scenario [1] and the accretion/merging one [2]– were proposed, that have long been influential for later observational and theoretical studies of disk and elliptical galaxies. Although observational studies of stellar halos in galaxies beyond the Local Group of galaxies have just recently started revealing structural and chemical properties of the halos [3][4], physical properties of globular cluster systems (GCSs) in these galaxies have long been investigated in much more details [5]. Wide-field imaging and spectroscopic studies with large ground-based telescopes (e.g., Keck 10m) have recently revealed GCS structures and kinematics in galaxies with different Hubble types [6]. Furthermore a growing number of theoretical/numerical studies have recently been accumulated which have investigated dynamical and chemical properties of GCs and GCSs based on admittedly realistic and self-consistent models of GC formation during galaxy formation and evolution [7][8]. In this review paper, we therefore try to derive physical meanings from the selected four observed properties of GCs and GCSs by comparing our numerical simulations of GC and GCS formation with latest observations.

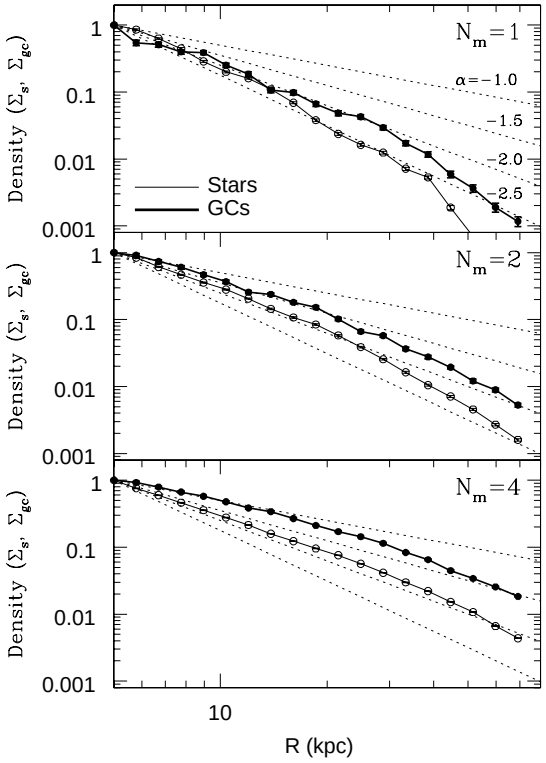

Fig. 1. Dependences of projected number distributions of stars (thin) and GCs (thick) in merger remnants (i.e., elliptical galaxies) on the total number of major merger events ($N_{\rm m}$) which an elliptical experienced during its formation (BF06). For clarity, the density distributions are normalized to their central values. Thin dotted lines represent power-law slopes (α) of $\alpha = -2.5$, -2.0, -1.5, and -1.0. Note that the density profiles of GCSs become flatter for larger $N_{\rm m}$, i.e. more mergers.

2 GCS density profiles

It has long been known that the radial density profiles of GCSs in elliptical galaxies (Es) vary with the total luminosities of their host galaxies [9]. If the projected GCS density profiles in Es with V-band absolute magnitudes of $M_{\rm V}$ are fitted to the power-law ones like $\Sigma_{\rm gc} \propto R^{\alpha_{\rm gc}}$, where R is the distance from the center of the host galaxy of a GCS, the power-law index $\alpha_{\rm gc}$ is smaller (i.e., the profiles are steeper) for larger $M_{\rm V}$ (i.e., fainter Es). Although two physical mechanisms – GC destruction by galactic tidal fields [10][11] and dynamics of galaxy merging (Bekki & Forbes 2006; BF06; [12]) – have been so far proposed for the origin of GCS density profiles, we focus on the latter case in this paper.

BF06 numerically investigated the structural properties of GCSs in Es formed from a sequence of major dissipationless galaxy merging and thereby

found that the radial density profiles of GCSs in Es become progressively flatter as the galaxies experience more major merger events (See Figure 1). The simulated profiles of GCSs are found to be well described as power-laws with $\alpha_{\rm gc}$ ranging from -2.0 to -1.0 in Es. They are flatter than, and linearly proportional to, the slopes ($\alpha_{\rm s}$) of the stellar density profiles. By applying a reasonable scaling relation between luminosities and sizes of galaxies to the simulation results, BF06 showed that $\alpha_{\rm gc} \approx -0.36 M_{\rm V} - 9.2$, $r_{\rm c} \approx -1.85 M_{\rm V}$, and $\alpha_{\rm gc} \approx 0.93 \alpha_{\rm s}$. These correlations between GCS profiles and their host galaxy luminosities are consistent reasonably well observations [13][9] which suggests that the origin of structural non-homology of GCSs in Es can be understood in terms of the growth of Es via major dissipationless galaxy merging.

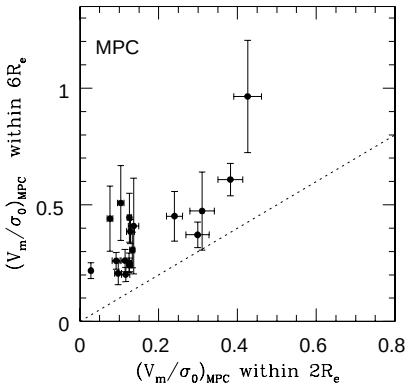

Fig. 2. Correlations between $(V_{\rm m}/\sigma_0)_{\rm MPC}$ estimated for $R \leq 2R_{\rm e}$ and those for $R \leq 6R_{\rm e}$ for metal-poor clusters (MPCs). These correlations are derived from 18 results of 6 major merger models with three different projections [18].

3 GCS kinematics in E/S0s

Recent observations on GCS kinematics in E/S0s have revealed that GCS kinematics can be quite diverse: GCSs in some galaxies like M87 [14] NGC 4472 [15] and NGC 5128 [16] show rotation whereas those in some galaxies such as NGC 1399 [17] do not. Bekki et al. (2005; B05; [18]) first tried to understand the observed diversity in GCS kinematics by numerically investigating GCS kinematics of E/S0s formed from major/minor galaxy merging. B05 demonstrated that both metal-poor cluster (MPCs) and metal-rich ones (MRCs) in Es formed from major mergers can exhibit significant rotation at large radii ($\sim$20 kpc) due to the conversion of initial orbital angular momentum into intrinsic angular momentum of the remnant.

Based on a wide parameter study of galaxy mergers, B05 found that MPCs show higher central velocity dispersions than MRCs for most major merger models. $V_{\rm m}/\sigma_0$ (where $V_{\rm m}$ and σ_0, are the GCS maximum rotational velocity and central velocity dispersion, respectively) ranges from 0.2– 1.0 and 0.1–0.9 for the MPCs and MRCs respectively, within $6R_{\rm e}$ for the remnant elliptical. Figure 2 shows an interesting result that does not depend on merger parameters: $V_{\rm m}/\sigma_0$ of MPCs within $6R_{\rm e}$ are greater than those of MPCs within $2R_{\rm e}$.

B05 also revealed the alignment of the major axes in 2D distributions between stars, GCs, and dark matter halos in the simulated Es. The aligned major axis between stars, GCs, and dark matter appears to be one of the principal characteristics of Es formed by major merging, which implies that *observational studies on 2D distributions of GCSs in Es can tell us about the shapes of their host dark matter halos*. We also showed in this meeting that the total masses of E/S0s estimated from the GCS kinematics can be much closer to the real masses than those from the PNe systems owing to less anisotropic velocity dispersion in GCSs, in particular, for face-on S0s. This suggests that (1) GCSs are better mass-estimators in E/S0s and (2) kinematical data sets of PNe systems in E/S0s [19] should be more carefully interpreted for the total masses of E/S0s. Although these simulations are not based on cosmological N-body ones, these results may well provide new insight on the origin of the observed diversity in GCS kinematics of E/S0s.

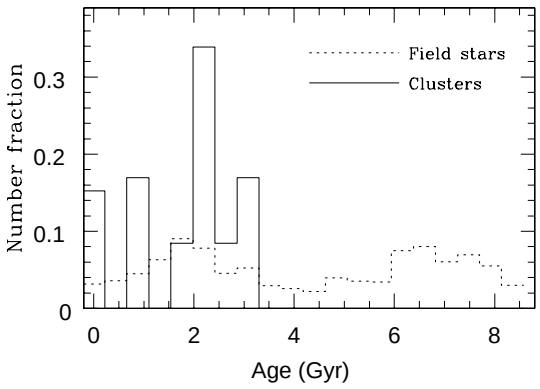

Fig. 3. The simulated age distributions of field stars (dotted) and clusters (solid) in the LMC at the present epoch [25]. For convenience, the normalized fraction of stars in each age bin is shown.

4 The age gap problem in the LMC

Possible candidates of young and metal-rich GCs were discovered in interacting and merging galaxies [20], and physical properties of these GCs have been discussed in different contexts of galaxy and GC formation, such as the observed color bimodality in GCSs in Es [9], the birth rate of young GCs as a function of time in M82 [21] and the age-metallicity relation of GCs in nearby interacting galaxies like the LMC and the SMC (e.g., Bekki et al. 2004; B04; [22]). In this paper, we focus on the LMC's GCS in which nearly all GCs are either very old ($\sim$ 13 Gyr) or younger than $3-4$ Gyr – the "age-gap" problem [23][24].

B04 and Bekki & Chiba (2005; [25]) challenged this age gap problem by investigating chemodynamical evolution of the LMC interacting both with the Galaxy and the SMC for a long time scale ($\sim$ 9 Gyr). They found that the first close encounter between the LMC and the SMC about 4 Gyr ago was the beginning of a period of strong tidal interaction witch likely induced dramatic gas cloud collisions, leading to an enhancement of the GC formation which has been sustained by strong tidal interactions to the present day. Figure 3, showing the simulated age distributions of field stars and GCs in a model, reveals that GC formation can be reactivated about $3-4$ Gyr ago, when the LMC can start its strong tidal interaction with the SMC. These results imply that the origin of the age gap can be closely associated with interaction histories of the LMC, the SMC, and the Galaxy.

5 Very massive star clusters

Very massive star clusters (VMSCs) such as ω Centauri, ultra-compact dwarfs (UCDs), and massive nuclear star clusters have unique characteristics that are quite different from those of "normal" GCs. For example, UCDs discovered in the Fornax and the Virgo clusters of galaxies [26][27][28] have intrinsic sizes of less than 100 pc, and have absolute $B-$band magnitudes ranging from -13 to -11 mag, which is more than 2 magnitudes brighter than the most massive GC in the Galaxy (i.e., ω Cen). Two physical mechanisms for the VMSC formation have been so far proposed: The "Galaxy threshing" scenario [29][30] in which VMSCs originate from nuclei of nucleated dwarf galaxies and the "cluster merging" one in which VMSCs are formed from merging of smaller star clusters in tidal tails of merging galaxies [31]. Although more details on physical properties of VMSCs have been recently revealed [32][33], it remains unclear which of the two scenarios is more convincing for the origin of VMSCs.

Here we discuss what we can learn from VMSC properties *if they were previously nuclei of nucleated galaxies.* Both dissipationless [34][35] and dissipative [36] formation scenario of stellar galactic nuclei have provided some interesting predictions on nuclear properties of galaxies [37]. Figure 4 shows the scaling relations between different physical parameters of merger remnants

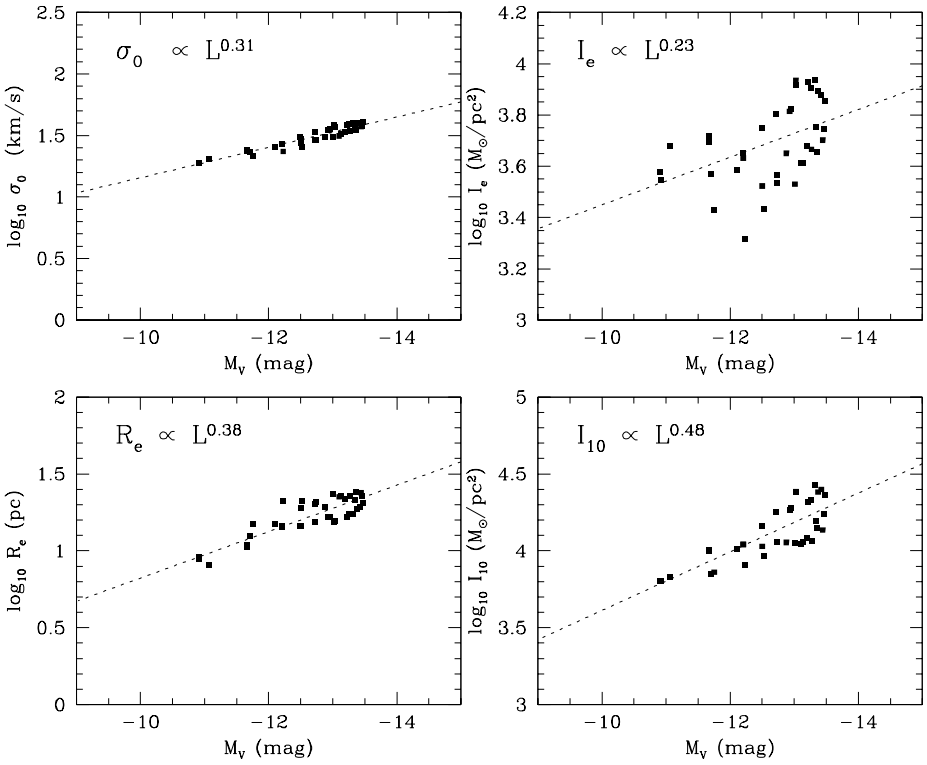

Fig. 4. Correlations of structural and kinematical parameters with $M_{\rm V}$ ($V-$band absolute magnitude) for the VMSCs in 40 models [22]. Projected central velocity dispersion (σ_0; *upper left*), half-light-averaged surface brightness (I_e; *upper right*), effective radius (R_e; *lower left*), and central surface brightness (I_{10}; *lower right*) are plotted against $M_{\rm V}$. Here the central surface brightness I_{10} is expressed as $0.1L/\pi/{R_{10}}^2$, where L, R_{10} are the total luminosity of a VMSC and the radius within which 10% of L is included, respectively. The best fit scaling relation for the VMSCs is derived for each panel using the least square fitting method and described as a *dotted* line with the derived relation (e.g., $\sigma_0 \propto L^{0.31}$).

of star clusters initially with the observed GC scaling relations [38]. The fact that the simulated relations deviate from the GC's ones implies that *the scaling relations of VMSCs can be used for understanding whether the stellar nuclei can be formed from merging of many smaller clusters in the central regions of galaxies* [39]. The dissipative nucleus formation model [37] has predicted the spread of ages and metallicities in stellar populations of stellar galactic nuclei and accordingly can be discussed in the context of the observed spread of ages and metallicities in ω Cen [32]. Thus dynamical and chemical properties of VMSCs can tell us about nucleus formation histories in galaxies.

6 Future works: Hierarchical galaxy formation and GCSs

Thus, structural, kinematical, and chemical properties of GCSs in galaxies have fossil information on dynamics of major/minor galaxy merging (e.g, angular momentum redistribution processes in merging), interaction histories of galaxies, and the formation histories of stellar galactic nuclei in dwarfs. Previous theoretical/numerical studies however did not discuss so extensively the observed correlations between GCS properties and their host ones [6] in the context of a hierarchical clustering scenario of galaxy formation. Several authors just recently have started their investigation on the GCS-host relations based on semi-analytic models [40] and high-resolution numerical simulations in ΛCDM models [41][42]. A number of observed GCS-host relations, such as the positive correlation between GCS metallicities and their host galaxy luminosities [6] have not been clearly explained by any galaxy formation scenarios. Since these GCS-host relations may have profound physical meanings on galaxy formation and evolution, it is doubtlessly worthwhile for future numerical simulations of GCS formation to explore the origin of these relations.

References

1. O.J. Eggen, D. Lynden-Bell, A.R. Sandage: ApJ, **136**, 748 (1962)
2. L. Searle, R. Zinn: ApJ, **225**, 357 (1978)
3. J. Dalcanton, R.A. Bernstein: AJ, **123**, 1328 (2002)
4. S. Zibetti, S.D.M. White, J. Brinkmann: MNRAS, **347**, 556 (2004)
5. W.E. Harris: ARA&A, **29**, 543 (1991)
6. J.P. Brodie, J. Strader: ARA&A in press (astro-ph/0602601) (2006)
7. K. Bekki, D.A. Forbes, M.A. Beasley, W.J. Couch: MNRAS, **335**, 1176 (2002)
8. O.Y. Gnedin: in this volume (2006)
9. K.M. Ashman, S.E. Zepf: in Globular cluster systems, Cambridge, U. K. ; New York : Cambridge University Press (1998)
10. H. Baumgardt: A&A, **330**, 480 (1998)
11. E. Vesperini, S. E. Zepf, A. Kundu, K.M. Ashman: ApJ, **593**, 760 (2003)
12. K. Bekki, D.A. Forbes: A&A, **445**, 485 (2006)
13. W.E. Harris: AJ, **91**, 822 (1986)
14. M. Kissler-Patig, K. Gebhardt: AJ, **116**, 2237 (1998)
15. S.E. Zepf, M.A. Beasley et al: AJ, **120**, 2928 (2000)
16. E.W. Peng, H.C. Ford, K.C. Freeman: ApJ, **602**, 705 (2004)
17. T. Richtler et al: AJ, **127**, 2094 (2004)
18. K. Bekki, M.A. Beasley, J.P. Brodie, D.A. Forbes, MNRAS, **363**, 1211 (2005)
19. A.J. Romanowsky, N.G. Douglas et al: Science, **301**, 1696 (2003)
20. B.C. Whitmore, F. Schweizer: AJ, **109**, 960 (1995)
21. R. de Grijs, N. Bastian, H.J.G.L. Lamers: MNRAS, **340**, 197 (2003)
22. K. Bekki, W.J. Couch, W. J. et al: **610**, L93 (2004)
23. G.S. Da Costa: in Haynes R., Milne D., eds, Proc. IAU Symp. 148, The Magellanic Clouds, Kluwer, Dordrecht, p183 (1991)
24. D. Geisler: in this volume (2006)

25. K. Bekki, M. Chiba: MNRAS, **356**, 680 (2005)
26. M.J. Drinkwater, M.D. Gregg et al: Nature, **423**, 519 (2003)
27. J.B. Jones, M.J. Drinkwater et al: AJ, **131**, 312 (2006)
28. S. Mieske, M. Hilker, L. Infante:, A&A, **418**, 445 (2004)
29. K. Bekki, W.J. Couch, M.J. Drinkwater: ApJ, **552**, L105 (2001)
30. K. Bekki, W.J. Couch, M.J. Drinkwater, Y. Shioya: MNRAS, **344**, 399 (2003)
31. M. Fellhauer, P. Kroupa: MNRAS, **330**, 642 (2002)
32. M. Hilker, A. Kayser, T. Richtler, P. Willemsen: A&A, **422**, L9 (2004)
33. M. Haşegan et al: ApJ, **627**, 203 (2005)
34. S.D. Tremaine, J.P. Ostriker, L. Spitzer, Jr: ApJ, **196**, 407 (1975)
35. R. Capuzzo-Dolcetta, A. Tesseri: MNRAS, **308**, 961 (1999)
36. K. Bekki, W.J. Couch, Y. Shioya: ApJL, in press (astro-ph/064340) (2006)
37. K. Bekki, W.J. Couch, M.J. Drinkwater, Y. Shioya, ApJ, **610**, L13 (2004)
38. S.G. Djorgovski, R.R. Gal et al: ApJ, **474**, L19 (1997)
39. P. Côte et al: 2006, ApJS in press (astro-ph/0603252) (2006)
40. M.A. Beasley, C.M. Baugh et al: MNRAS, **333**, 382 (2002)
41. K.L. Rhode, S.E. Zepf, M.R. Santos: ApJ, **630**, L21 (2005)
42. K. Bekki, H. Yahagi, D.A. Forbes: submitted to ApJL (2006)